Hydrodynamics of Droplet Coalescence

Dirk G. A. L. Aarts,[1,*] Henk N. W. Lekkerkerker,[1] Hua Guo,[2] Gerard H. Wegdam,[2] and Daniel Bonn[2,†]

[1]*Van't Hoff Laboratory, Debye Institute, Utrecht University, Padualaan 8, 3584 CH Utrecht, The Netherlands*

[2]*Van der Waals–Zeeman Institute, University of Amsterdam, Valckenierstraat 65, 1018 XE Amsterdam, The Netherlands*

(Received 17 May 2005; published 11 October 2005)

We study droplet coalescence in a molecular system with a variable viscosity and a colloid-polymer mixture with an ultralow surface tension. When either the viscosity is large or the surface tension is small enough, we observe that the opening of the liquid bridge initially proceeds at a constant speed set by the capillary velocity. In the first system we show that inertial effects become dominant at a Reynolds number of about 1.5 ± 0.5 and the neck then grows as the square root of time. In the second system we show that decreasing the surface tension by a factor of 10^5 opens the way to a more complete understanding of the hydrodynamics involved.

DOI: 10.1103/PhysRevLett.95.164503 PACS numbers: 47.20.Dr, 47.55.Dz, 82.70.Dd

The seemingly simple problem of the coalescence of droplets was already studied at the end of the 19th century [1]. Coalescence intervenes in many physical situations. For example, the droplet size distribution in rain is (among other processes) determined by it [2]. A detailed understanding of coalescence is important in a large number of industrial applications, such as emulsion stability, ink-jet printing, coating applications, and the dynamics of multiphase flows [3]. The last few years have witnessed a renewed interest in the breakup of free-surface flows under the influence of surface tension [4]. Notably, significant progress has been made in the study of the hydrodynamic singularities that occur in these problems. For the coalescence of a droplet, at the moment of contact, a singularity occurs due to the inversion of one of its two radii of curvature. Detailed theory [5] and numerics [6] have been able to capture the singularity, and an understanding of the hydrodynamics of the coalescence has been developed. However, experimentally, because of the rapidity of the phenomenon, very few quantitative studies of the initial stages of coalescence exist.

In this Letter we provide a detailed experimental study of the coalescence of two droplets and of a droplet with its bulk fluid phase, and compare with the theoretical predictions. We succeed in observing purely viscous coalescence, where the radius R of the liquid bridge grows linearly with time t, as opposed to inertial coalescence for which $R \propto \sqrt{t}$. The latter has recently been observed in other experiments [7,8]. We achieve in observing the linear dependence not only by increasing the viscosity considerably as, for example, very recently shown in [9,10], but also by decreasing the surface tension by 5 orders of magnitude. To this end, we use a molecular system with a variable (high) viscosity and a colloid-polymer mixture with an ultralow surface tension [11,12].

To appreciate the difficulty of observing purely viscous coalescence, we first discuss the relevant length and time scales. After a connecting bridge between the two surfaces has formed, the opening speed of this bridge results from a competition between the capillary forces driving the coalescence, and the viscous forces slowing it down. Equating these two forces (i.e., setting the capillary number to unity) leads to a dependence of the radius of the bridge R on time t as $R(t) \sim \gamma/\eta t$, where γ is the surface tension and η the viscosity. This coalescence mechanism leads to large speeds for ordinary liquids: for water the capillary velocity is $\gamma/\eta \sim 70\ \mathrm{ms}^{-1}$. The full theory predicts only logarithmic corrections to the above scaling arguments [5]:

$$R(t) = -\frac{\gamma t}{\pi \eta} \ln\left(\frac{\gamma t}{\eta R_0}\right), \tag{1}$$

with R_0 the radius of the undistorted droplet. We show below that in experiment these corrections are not observed.

Whether it is mainly viscous or inertial forces that govern the coalescence dynamics is determined by the relative importance of these two forces, i.e., by the Reynolds number Re. Using the capillary velocity as the characteristic speed and R as the characteristic size, it reads $\mathrm{Re} \sim \rho\gamma R/\eta^2$, with ρ the fluid density; one anticipates viscous coalescence for $\mathrm{Re} < 1$, and inertial coalescence for $\mathrm{Re} > 1$. If we assume that the crossover between the two regimes happens at $\mathrm{Re} \sim 1$ (as will be verified experimentally below), this sets a characteristic length and time scale beyond which inertia should become important; it follows that $R_\eta = \eta^2/\rho\gamma$, and $t_\eta = \eta^3/\rho\gamma^2$. Putting in the corresponding numbers for water, we find $R_\eta \sim 15$ nm and $t_\eta = 10^{-10}$ s. Clearly, for water there is no hope of observing the viscous regime, and the coalescence is from a practical point of view always inertial. The only options to observe the viscous regime are therefore to increase the viscosity or decrease the surface tension. Here, we pursue for the first time both options, where the first method also shows at what lengths inertial terms become dominant and the second method allows observing the viscous coalescence for longer times and in greater detail.

In the first series of experiments—dealing with the increase of viscosity—we use a new generation rapid

camera (Phantom V7) allowing us to take 120.000 frames per second to study the coalescence of two droplets. To vary the viscosity of the fluid over several orders of magnitude, we use silicon oils (Rhodorsil) of variable viscosity: $0.005 < \eta < 1$ Pa s. The silicon oils have a constant and relatively low surface tension (20 mN m^{-1}) and a constant density (970 kg m^{-3}). The constancy is important in order to vary only a single parameter in the problem.

The experiments were done by bringing the free surfaces of a pendant and a sessile drop (made with a syringe pump attached to 4 mm diameter capillaries) in each other's close vicinity, and simply waiting for the coalescence event to happen. Figure 1 shows a typical sequence of events, which underlines the rapidity of the phenomenon once more. From these images, $R(t)$ was obtained. The results for the highest viscosities are shown in Fig. 2(a). In Fig. 2(b) we have rescaled the radius with R_0 and the time with the viscous time $\tau_v = \eta R_0/\gamma$: the data collapse on a straight line. We do not find deviations from a straight line; i.e., the theoretically predicted logarithmic correction is not observed, possibly since this is an asymptotic result estimated to be valid for $R \lesssim 0.03 R_0$ [5]. Our optical resolution does not allow us to probe that regime in sufficient detail, as shown in the inset of Fig. 2(a). The slope of the line through the origin is 0.55 ± 0.06, showing that the opening speed of the neck is close to half the capillary speed. The choice of the beginning of the coalescence event ($t = 0$) poses some problems. It was therefore necessary to align the camera precisely at the level of the coalescing droplets, in order not to observe any "shadow effect" of one droplet onto the other. Once this problem was solved, fitting with $t = 0$ as an adjustable parameter or choosing the frame corresponding to $t = 0$ directly yielded similar results. It seems plausible that the observed finite initial contact radius in the experiments of Thoroddsen *et al.* [10] is due to the shadow effect. The main difference between the values reported here and in Ref. [10] is that our opening speed is a factor of 2 smaller. The speed reported in [10] is *higher* than the capillary speed by more than 20%. One might expect shock waves to form at speeds larger than the capillary speed; however, there is no indication in either of the experiments that this is the case.

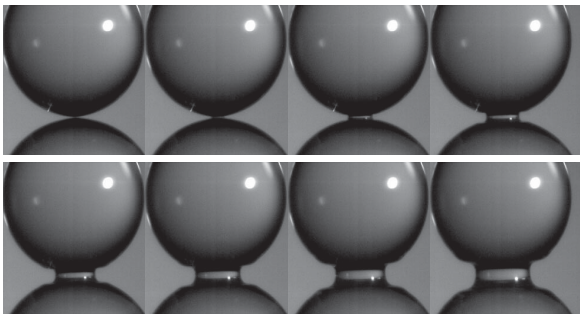

FIG. 1. Coalescence of two water drops; eight consecutive images taken at 11.200 frames/s at a resolution of 256×256 pixels. The image size is 5.12 mm by 5.12 mm and $R_0 = 2$ mm.

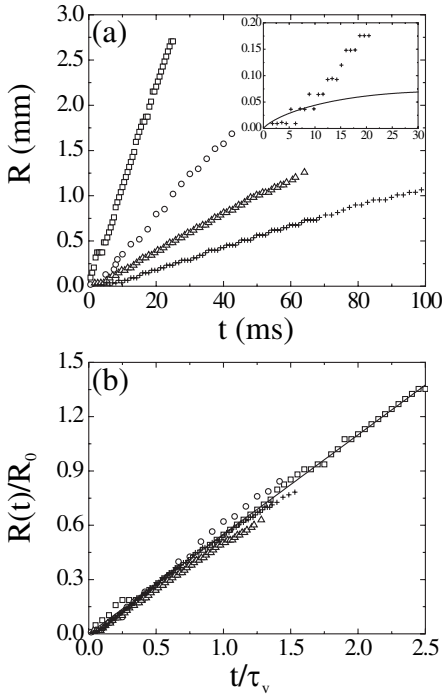

FIG. 2. The time evolution of the radius of the neck for high viscosity fluids. Squares: 100 mPa s; circles: 300 mPa s; triangles: 500 mPa s; plusses: 1 Pa s. The inset in (a) zooms in on the data for the highest viscosity close to $t = 0$ compared to the prediction by Eggers *et al.* [5] (full curve). (b) The data collapse after scaling with R/R_0 and t/τ_v. The full line is for $0.55\gamma/\eta$.

For the lowest-viscosity fluids, the fluid inertia does become important as can be observed in Fig. 3. In this case no analytical theory exists for $R(t)$. However, Eggers *et al.* [5] propose a scaling argument similar to the one above. For equating capillary and inertial forces, it is not sufficient to set the Weber number ($\mathrm{We} = \rho u^2 L/\eta$) to unity, since the capillary forces driving the coalescence are not simply γ/R but rather $\gamma R_0/R^2$ [5,6]. Equating this to the inertial forces, they find

$$R \sim \left(\frac{\gamma R_0}{\rho}\right)^{1/4} \sqrt{t}. \tag{2}$$

This $\sqrt{t}$ dependence was subsequently observed in the numerical simulations of an inviscid fluid by Duchemin *et al.* [6], who also found that the numerical prefactor (which does not follow from such a simple scaling argument) is 1.62. However, in the subsequent experiments of Wu *et al.* [7], a lower prefactor was found: 1.09 for water. When we rescale the time with the inertial time $\tau_i = \sqrt{\rho R_0^3/\gamma}$ [7], all the data collapse [Fig. 3(b)] and we find the following prefactors: water, 1.14; 5 mPa s silicon oil, 1.24; and 20 mPa s silicon oil, 1.11; these are in agreement with the other experiments [7,10,13], but in disagreement with the simulations [6]. In the simulations repeated connections are observed, possibly explaining the discrepancy. The crossover between the two regimes is clearly visible

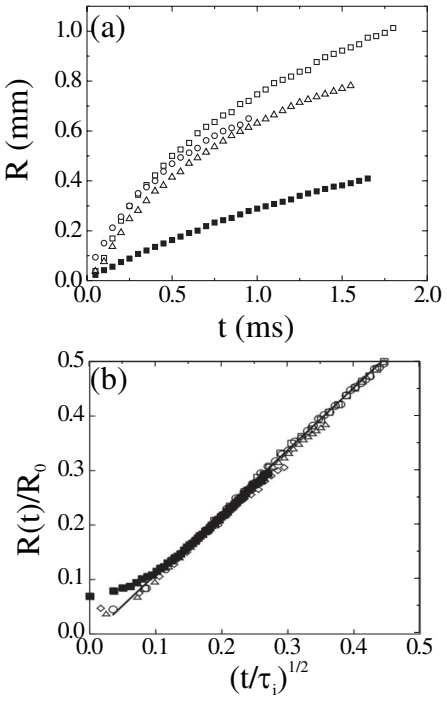

FIG. 3. The time evolution of the radius of the neck for low viscosity fluids. Open squares: water; circles: 5 mPa s; triangles: 20 mPa s; filled squares: 50 mPa s. In (b) the data collapse after scaling with R/R_0 and t/τ_i. The full line has a slope of 1.2. For the system of 50 mPa s the crossover between the viscous and inertial regimes can be observed; the curve has been shifted upwards artificially for the late-time behavior to coincide.

for the silicon oil of viscosity 50 mPa s, and happens at a crossover time of 450 ± 150 μs, leading to a crossover Reynolds number of $\mathrm{Re}_c = 1.5 \pm 0.5$; these experiments therefore in addition allow us to determine Re_c.

In all of the experiments on simple liquids, the coalescence is still so rapid that the other hydrodynamic processes involved are difficult to study. By strongly decreasing the surface tension, however, we succeed in observing the viscous coalescence, and it becomes possible to study in detail the other processes as well. A 5 orders of magnitude decrease in γ with respect to the system described above is achieved by preparing a mixture of colloids [50 nm in diameter, fluorescently labeled poly(methyl methacrylate) latex particles] and slightly smaller polymers (polystyrene of $M_w = 2.33 \times 10^5$ g/mol from Fluka) in decalin [11]. Because of a depletion interaction this system spontaneously phase separates into a colloid-rich phase (a colloidal ''liquid'') and a polymer-rich phase (a colloidal ''gas'') at sufficiently high polymer and colloid concentrations [14,15]. It then behaves as a two fluid system, with an extremely small surface tension. In the present work the surface tension is 0.16 μN/m as compared to 20 mN/m for the silicon oils. The surface tension has been measured by determining the capillary length (analyzing the colloidal ''gas-liquid'' interfacial profile near a vertical wall) and by analyzing the capillary wave spectrum [11,12]. Droplets are produced by simply shaking the container. Since the colloids are fluorescent, the colloidal liquid appears bright. Furthermore, the colloidal liquid is the heavier and thus the lower phase. This system allows one to study two different situations: the coalescence of colloidal gas and of colloidal liquid droplets with their corresponding bulk phases. Because of the viscosity contrast between the two phases, this is not a symmetrical situation: the viscosity of the colloid-rich phase is 31 mPa s, whereas that of the polymer-rich phase is 8 mPa s.

Figure 4 shows the coalescence for both cases, as observed directly by laser scanning confocal microscopy (LSCM). Transmission light microscopy has been used as well, allowing for 50 frames/s instead of 1 frame/s with LSCM. Figure 5 shows $R(t)$ obtained from light microscopy; again a linear behavior is found, as would be expected for viscous coalescence. The impressive observation is that both events are orders of magnitude slower than the coalescence of the silicon oils: typical speeds are a few $\mu\mathrm{m\,s^{-1}}$, about 10 000 times slower than the slowest coalescence in the first series of experiments. Furthermore, one expects that inertial terms become important at $R_\eta = 6$ m for the colloidal liquid droplets, which is 2 orders of magnitude larger than in the molecular system with the highest viscosity. Quantitatively, the speeds are 5.7 $\mu\mathrm{m\,s^{-1}}$ for the coalescence of the polymer-rich phase and 2.1 $\mu\mathrm{m\,s^{-1}}$ for the coalescence of the colloid-rich phase. From γ/η we expect velocities of 20 $\mu\mathrm{m\,s^{-1}}$ for the gas and 5.2 $\mu\mathrm{m\,s^{-1}}$ for the liquid droplets without taking the viscosity of the outer fluid into account. We thus observe prefactors to the capillary velocity of 0.3 for gas and 0.4 for liquid droplets. This is similar to the value of 0.55 found above for the coalescence in air. These results obtained in very different systems then allow for the conclusion that the observed coalescence velocities are, indeed, set by the capillary velocity. Furthermore, in the colloidal system the coalescence is slowed down by the viscosity of the surrounding fluid as well, even such that

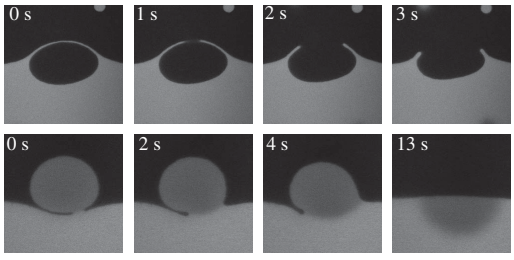

FIG. 4. LSCM images of droplet coalescence in a phase-separated colloid-polymer mixture. Shown are a polymer-rich droplet ($R_0 = 30$ μm, top row) and a colloid-rich droplet ($R_0 = 15$ μm, bottom row) coalescing with their bulk phases. In the bottom row we have partially bleached the dye of the colloids in the droplet, which allows following the extrusion of droplet material into the bulk phase; see also the accompanying movie [17]. Note the typical shape of the retracting interfaces, which is similar to predictions in [5].

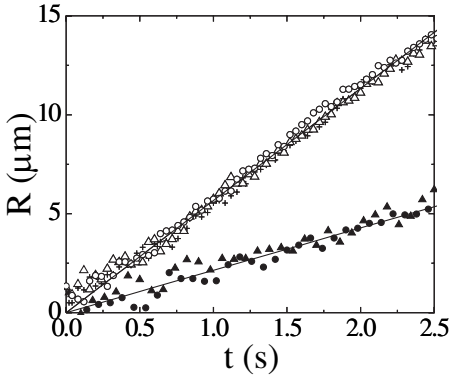

FIG. 5. The time evolution of the radius of the neck in a colloid-polymer mixture for polymer-rich gas droplets (open symbols: three different events with $R_0 = 16$, 17, and 18 μm) and colloid-rich liquid droplets (closed symbols: two different events with $R_0 = 15$ and 17 μm). Full curves are linear fits to the data.

the gas bubble is slowed down more by its relatively high viscous surrounding than the liquid droplet.

Besides allowing us to observe low Reynolds number coalescence, the colloid-polymer system opens the way to a more complete understanding of the hydrodynamics involved. In the final stage of drainage of the thin film intervening between droplet and bulk phase, a liquid bridge forms. In order for this to occur, van der Waals forces have been invoked in molecular fluids [16]. However, the van der Waals forces are very small in our system, as both phases have very similar dielectric constants. It is evident, especially from the movie accompanying Fig. 4, that the intrinsic dynamic roughness of the interface plays a more important role than the intermolecular forces [12]. Second, the surface energy gained in coalescence is transformed into kinetic energy of the liquid; however, it is much less clear what the flow pattern is and consequently where the droplet material goes. This can again be studied directly in this system by bleaching the fluorescence of either the droplet or the bulk; for the event in the bottom row of Fig. 4 we have partially bleached the dye of the colloids inside the droplet and as a result are able to follow the coalescence all the way into the bulk phase. Clearly, the interfaces first retract, followed by extrusion of the droplet material into the bulk phase. The material in the droplet forms a hemisphere, which subsequently spreads through diffusion. Finally, the drainage of the film can be studied directly from the microscopy images, as can the probability of coalescence as a function of the distance between the two interfaces; a detailed analysis of these phenomena are beyond the scope of this Letter, and will be reported elsewhere.

In summary, we have demonstrated experimentally that the coalescence dynamics of droplets is driven by surface tension, and slowed down by viscosity for low and by inertia for high Reynolds numbers. In the viscous regime, the opening speed is set by the capillary velocity γ/η, and in the range studied here no signs of the logarithmic correction of [5] are observed. In the inertial regime, the speed can be obtained by equating capillary and inertial forces with a proportionality constant very close to unity. The colloid-polymer system investigated here allows one to study viscous coalescence in detail, notably the other hydrodynamic processes, and opens the way for a more complete understanding of droplet coalescence.

We thank S. Thoroddsen for insightful remarks, M. Schmidt for useful discussions, and R. Dullens for particle synthesis. This work is part of the research program of the *Stichting voor Fundamenteel Onderzoek der Materie* (FOM), financially supported by NWO.

*Electronic address: d.g.a.l.aarts@chem.uu.nl
†Also at Laboratoire de Physique Statistique, Ecole Normale Superieure, 24, Rue Lhomond, F-75231 Paris Cedex 05, France.

[1] J. Thomson and H. Newall, Proc. R. Soc. London **39**, 417 (1885).
[2] A. Brandes, G. Zhang, and J. Vivekanadan, J. Appl. Meteorol. **43**, 461 (2004).
[3] A. Frohn and N. Roth, *Dynamics of Droplets* (Springer, Berlin, 2000).
[4] J. Eggers, Rev. Mod. Phys. **69**, 865 (1997).
[5] J. Eggers, J. R. Lister, and H. A. Stone, J. Fluid Mech. **401**, 293 (1999).
[6] L. Duchemin, J. Eggers, and C. Josserand, J. Fluid Mech. **487**, 167 (2003).
[7] M. Wu, T. Cubaud, and C. Ho, Phys. Fluids **16**, L51 (2004).
[8] A. Menchaca-Rocha, A. Martínez-Daávalos, R. Núñez, S. Popinet, and S. Zaleski, Phys. Rev. E **63**, 046309 (2001).
[9] W. Yao, J. Maris, P. Pennington, and G. Seidel, Phys. Rev. E **71**, 016309 (2005).
[10] S. T. Thoroddsen, K. Takehara, and T. G. Etoh, J. Fluid Mech. **527**, 85 (2005).
[11] D. G. A. L. Aarts and H. N. W. Lekkerkerker, J. Phys. Condens. Matter **16**, S4231 (2004).
[12] D. G. A. L. Aarts, M. Schmidt, and H. N. W. Lekkerkerker, Science **304**, 847 (2004).
[13] S. T. Thoroddsen (private communication).
[14] S. Asakura and F. Oosawa, J. Chem. Phys. **22**, 1255 (1954).
[15] A. Vrij, Pure Appl. Chem. **48**, 471 (1976).
[16] N. Chen, T. Kuhl, R. Tadmor, Q. Lin, and J. Israelachvili, Phys. Rev. Lett. **92**, 024501 (2004).
[17] See EPAPS Document No. E-PRLTAO-95-050542 for the coalescence of a liquid droplet. The movie has dimensions 55×55 μm^2. The playback rate is about 5 times real time. The interfaces are clearly dynamically rough due to thermal energy. The dye inside the liquid droplet has been partially bleached and the coalescence event can therefore be followed even into the bulk phase. There, the liquid material spreads through particle diffusion. This document can be reached via a direct link in the online article's HTML reference section or via the EPAPS homepage (http://www.aip.org/pubservs/epaps.html).